Res Chem Intermed (2015) 41:4293–4310
DOI 10.1007/s11164-014-1530-z

Esterification and amidation for grafting long aliphatic chains on to cellulose nanocrystals: a comparative study

Abdelkader Bendahou · Abdelghani Hajlane · Alain Dufresne · Sami Boufi · Hamid Kaddami

Received: 13 February 2013 / Accepted: 1 January 2014 / Published online: 11 January 2014

Abstract Heterogeneous modification of cellulose nanocrystals (CNC) has been achieved by using esterification and amidification to attach long aliphatic chains. Long-chain aliphatic acid chlorides and amines were used as grafting reagents. Surface grafting with acyl chains was confirmed by Fourier-transform infrared spectroscopy, elemental analysis, and X-ray photoelectron spectroscopy. It was found that the degree of substitution (DS) of the surface is highly dependent on the method of modification. Irrespective of grafting approach, the modified CNC was found to be hydrophobic after modification, as attested by contact angle measurement. The main emphasis was on the correlation between DS and the extent of surface grafting.

Keywords Cellulose nanocrystals · Surface modification · Grafting · Esterification · Amidification

A. Bendahou · A. Hajlane · H. Kaddami (✉)
Laboratoire de Chimie Organométallique et Macromoléculaire – Matériaux Composites, Faculty of Sciences and Technologies of Marrakesh, Cadi Ayyad University, Avenue Abdekrim Elkhattabi, BP549, Marrakech, Morocco
e-mail: hkaddami@yahoo.fr; h.kaddami@uca.ma

A. Dufresne
The International School of Paper, Print Media and Biomaterials (Pagora), Grenoble Institute of Technology, BP65, 38402 Saint Martin d'Hères Cedex, France

S. Boufi
Laboratoire Sciences des Matériaux et Environment, LMSE, University of Sfax, BP 802-3018, Sfax, Tunisia

Introduction

During the last decade there has been growing interest in the use of nanosized cellulose for reinforcement of polymer-based nanocomposites. Its incorporation within a polymer matrix at a level below 10 % (*w*/*w*) results in a substantial increase in stiffness and mechanical strength [1]. The high aspect ratio of the nanofibres, their high crystallinity, Young's modulus, and strength, and their tendency to form continuous networks result in huge improvement of mechanical properties [2]. Furthermore, given the nanosized scale of the reinforcement, less than the half the wavelength of the visible light, high transparency is expected.

Among nanosized cellulose, cellulose nanocrystals (CNC) have attracted much interest. These rod-like nanocrystals, which are extracted from fibres after complete dissolution of non-crystalline fractions, are 5–20 nm wide and up to 1 μm long, depending on the source of the cellulose and hydrolysis conditions [3]. A recent review reported the properties and application of CNC in nanocomposites [4]. However, even if the high reinforcement potential of cellulose nanofillers has been well established by numerous reports [4], this property depends on good dispersion of the nanofiller in the host polymer matrix during processing of the nanocomposite, which is not straightforward for two reasons:

- the nanoscale dimensions of the CNC result in an inherently large specific surface area (more than 100 m^2/g) which favours the tendency of the CNC to aggregate into bundles; and
- the inherently high hydrophilicity of the CNC, which arises from the high density of hydroxyl groups on their surface, restricts use of these rod-like nanoparticles to aqueous solutions or dispersions and hinders efficient dispersion in non-polar polymers or non aqueous solvents.

To prevent CNC from aggregating and to improve their dispersion and compatibility within the host matrix, modification of the cellulose surface has seemed to be one of the most promising solutions. Furthermore, this approach enables use of the melt-processing method, which is essential for production of bulky nanocomposites. Most reported investigations dealing with use of CNC for reinforcement are limited to waterborne polymer latex, enabling easy mixing of the CNC suspension with the polymer dispersion without any need to remove the CNC from the water. Several authors have described covalent derivatization of the cellulose surface at a nanometric level. Methods include acetylation [5], esterification [6], silylation [7], and coupling with *N*-alkyl isocyanate [8]. Polymer grafting of CNC by either the "grafting on to" [9] or "grafting from" [10] approach has also been investigated and revealed to be a promising way of improving both the compatibility of CNC and dispersion in a hydrophobic matrix [11]. It has, for example, been shown that PLA-grafted CNC, produced by ring-opening polymerization (ROP), ensured dispersion of the nanofiller via melt-blending, resulting in greater stiffness of the composite [12].

In this work, two approaches have been used for surface modification of CNC: esterification with acid chlorides or amidification with aliphatic amines after TEMPO oxidation of the CNC. The former was performed toluene after solvent exchange whereas the later was performed directly in water without any need to remove CNC

from the aqueous medium in which it was colloidally stable. Modification of the surface was confirmed by Fourier-transform infrared (FTIR) and X-ray photoelectron (XPS) spectroscopy and elemental analysis. The effect of the modification on the surface properties of the nanoparticles was analysed by measurement of contact angle.

Experimental

Materials

Sulfuric acid (95 %), triethylamine (TEA, 99.5 %), toluene (99.8 %), acetone (99 %), hexanoyl chloride (C6; 98 %), lauroyl chloride (C12; 98 %), stearoyl chloride (C18; 98.5 %), 2,2,6,6-tetramethylpiperidine-1-oxyl (TEMPO), 4-amino TEMPO, sodium bromide, sodium hypochlorite, *N*-(3-dimethylaminopropyl)-*N*′-ethylcarbodiimide hydrochloride (EDAC), and *N*-hydroxysuccinimide (NHS), were all purchased from Sigma–Aldrich, and used as received.

n-Propylamine (A3; 99 %), *n*-octylamine (A8; 99 %), dodecylamine (A12; 98 %), and octadecyl amine (A18; 90 %) were obtained from Fluka.

Preparation of CNC

CNC was prepared from date palm by acid hydrolysis, by use of procedure reported in detail elsewhere [13].

Esterification of the CNC

Surface modification of CNC was performed in toluene in a round-bottomed flask under reflux (6 h) and with constant mechanical stirring. The toluene suspension was obtained by successive solvent exchange and centrifugation (water to acetone, acetone to methyl ethyl ketone and, finally, methyl ethyl ketone to toluene, four times for each exchange).

CNC (2 g) were mixed with triethylamine (5 mL) and the acyl chloride (5.2 mL for hexanoyl, 8.8 mL for lauroyl, or 12.5 mL for stearoyl chloride). Triethylamine was used as catalyst and neutralizing agent for HCl formed during the reaction [9]. The modified CNC were submitted to Soxhlet extraction, first with ethanol and then with dichloromethane, for 24 h. CNC modified with hexanoyl chloride, lauroyl chloride, and stearoyl chloride were denoted WAG6, WAG12, and WAG18, respectively, whereas unmodified CNC was denoted WRPd.

Coupling of amines with oxidized CNC

Reaction of CNC by TEMPO-mediated oxidation

CNC (0.32 g; 2 mmol) were dispersed in 100 mL distilled water. Sodium bromide (0.1 g; 1.0.00 mmol) and the radical TEMPO (5 mg; 0.032 mmol) were then added after stabilization of the temperature (4 °C) and at pH $\sim$10. The desired amount of

sodium hypochlorite was introduced dropwise to maintain the pH at 10. The volume of sodium hypochlorite added was recorded against time, enabling the kinetics of the reaction to be followed. The pH was controlled by addition of 1 M NaOH. When the pH was stabilized (after reaction for 5 h) reaction was regarded as complete. Methanol (5 mL) was then added to destroy residual NaOCl and the pH was adjusted to 7 with 1 M HCl. The water-insoluble fraction was recovered by centrifugation and washed thoroughly with distilled water. The oxidized CNC were dialyzed against distilled water and concentrated by freeze-drying.

Coupling reaction with amine

The coupling reaction between oxidized CNC and amine molecules was performed in a 80:20 water–ethanol. Amine molecules were added to oxidized CNC aqueous suspension with a solid content of 0.2 wt% (2 g), followed by *N*-hydroxysuccinimide (NHS; 2 mol NHS/mol carboxyl group) and 1-ethyl-3-(3-dimethylaminopropyl) carbodiimide (EDAC; 2 mol EDAC/mol carboxyl group). The pH was adjusted to 7.5–8 by addition of 0.5 M HCl and 1 M NaOH solutions. The resulting suspension was stirred for 24 h at 55 °C and, finally, the cellulose derivatives were precipitated by adding excess ethanol. After cooling to room temperature the mixture was centrifuged. The solid product was recovered, washed several times with distilled water and re-centrifuged, to eliminate the EDAC, the NHS, and unreacted amine. The functionalized nanoparticles were then dispersed in water, dialyzed against distilled water for four days, then freeze-dried. Finally, the modified nanocrystals were submitted to Soxhlet extraction, first with ethanol and then with dichloromethane, each for 24 h. All the amines used, and the EDAC and NHS, were soluble in ethanol.

Characterization

Atomic force microscopy (AFM)

For AFM observations, the aqueous suspension of cellulose nanoparticles was diluted to 0.01 mg/mL with distilled water. A drop of the suspension was deposited on a mica sheet (Agar) and the water was evaporated. The AFM images were recorded in tapping mode (TM) with a nanoscope IIIa microscope from Veeco Instruments. Both height and phase images of 512 × 512 data points were recorded in an ambient atmosphere, at room temperature, by use of silicon probes with a spring constant of 24–52 N/m, a resonance frequency in the 264–339 kHz range, and a typical radius of curvature of 10–15 nm.

FTIR analysis

A Perkin–Elmer Paragon 1000 FTIR spectrometer equipped with Spectrum software was used to perform FTIR analysis. The spectra were obtained by preparing dried KBr powder pellets containing 1 % *w*/*w* of the investigated samples. Spectra were recorded between 400 and 4000 cm^{-1}, with 4 cm^{-1} resolution and accumulation of 16 scans.

X-ray photoelectron spectroscopy

XPS measurements were performed on the dried pellets of powdered CNC, before and after grafting, by use of a Kratos AXIS Ultra photoelectron spectrometer. Pellets were prepared from dried powder then washed with chloroform to remove contaminants and then stored in a vacuum oven for a few hours at 40 °C before analysis. The XPS experiments were conducted at room temperature with a base pressure of 10^{-9} mbar. The monochromatic Al K X-ray source was operated at 300 W (15 kV, 20 mA). Low-resolution survey scans were obtained with a 1 eV step and 80 eV analyser pass energy; high-resolution spectra were acquired with a 0.1 eV step and 20 eV analyser pass energy. Atomic concentrations were calculated from the photoelectron peak areas by use of Gaussian–Lorentzian deconvolution. The carbon 1s spectra were resolved into the different contributions of bonded carbons, namely, carbon without oxygen bonds (C–C and C–H), carbon with one oxygen bond (C–O), carbon with two oxygen bonds (O–C–O), and carbon with three oxygen bonds (O–C=O). The chemical shifts were taken from the literature and the spectra were charge-corrected by setting the carbon-without-oxygen-bond contribution in the C1s emission to 285.0 eV [14].

Contact angle measurements

The dynamic contact angle of sessile drops of water on the CNC was measured with an OCA20 automated and software-controlled video-based contact angle meter (Data-Physics Instruments, Filder-stard, Germany). All measurements were conducted at room temperature (22 °C). Three different liquids, with different dispersive and polar surface tensions, were used to determine the surface energy of CNC. The drop volume was between 5 and 10 μL, and smooth surface nanocrystal samples were obtained by compacting the powder under a pressure of 10 metric tons by use of a press. Contact angle measurements were performed on CNC samples before and after modification.

The Owens–Wendt approach [19] was used to calculated the dispersive and polar contributions to the surface energy of the CNC samples by use of Eq. (1):

$$\gamma_L(1+\cos\theta) = 2\sqrt{\gamma_S^D\gamma_L^D} + 2\sqrt{\gamma_S^P\gamma_L^P} \tag{1}$$

where γ, γ^d, and γ^p are the total, dispersive, and polar surface energy, respectively. Subscripts L and S refer to the liquid drop and the solid surface, respectively, and θ denotes the contact angle between the solid substrate and the liquid drop.

According to Eq. (1):

$$\frac{\gamma_L(1+\cos\theta)}{2\sqrt{\gamma_L^D}} = \frac{\sqrt{\gamma_S^P\gamma_L^P}}{\sqrt{\gamma_L^D}} + \sqrt{\gamma_S^D} \tag{2}$$

where $(\gamma_s^P)^{0.5}$ and $(\gamma_S^D)^{0.5}$ are the slope and the *y*-axis intercept, respectively, for each of the materials tested. The total surface energy of the CNC is easily obtained by use of the equation:

$$\gamma_S = \gamma_S^D + \gamma_S^P \tag{3}$$

Carboxyl content

The carboxyl content of oxidized CNC samples was determined by conductimetric titration. The CNC samples (50 mg) were suspended in 15 mL 0.01 M hydrochloric acid solution. The titration curves showed the presence of a strong acid, corresponding to excess HCl, and a weak acid, corresponding to carboxyl content. The degree of oxidation (DO), is given by Eq. (4):

$$\mathrm{DO} = \frac{162 \times C \times (V2 - V1)}{w - 36 \times C \times (V2 - V1)} \tag{4}$$

where C is the NaOH concentration (mol/L), V_1 and V_2 are the amount of NaOH needed for the neutralization of the blank and the CNC suspension, respectively, and w (g) the weight of the oven-dried sample.

Elemental analysis

Duplicate elemental analysis was performed at the Laboratoire Central d'Analyses de Vernaison, France (CNRS). This technique is based on atomic absorption of the elements investigated. The carbon, nitrogen, and oxygen content of the CNC were measured independently.

Results and discussion

Although several papers dealing with heterogeneous esterification of CNC have been published [15] we chose to perform surface esterification of CNC with acid chlorides under heterogeneous conditions for two reasons:

- first, to compare, in terms of the DS, the efficiency of grafting based on surface esterification in organic solvent and amidification in aqueous medium; and
- second, to determine the effect of each modification on the surface properties of the CNC.

Characterization of the CNC

The morphology of CNC extracted from the rachis of the date palm tree was assessed by AFM and TEM observation. Values around 260 ± 20 and 6 ± 2 nm, respectively, were obtained for the length and diameter, giving an aspect ratio of approximately 43. Figure 1 shows an AFM micrograph of CNC extracted from the rachis of the date palm tree.

Modification of the CNC by esterification with long chains acid chloride

The FTIR spectra of the CNC before and after modification with acid chloride are shown in Fig. 2. Pristine CNC are characterized by the typical bands of the cellulose skeleton in the region 1000–1200 cm^{-1} assigned to the carbohydrate ring. Bands at

1160, 1110, and 1060–1030 cm^{-1} correspond to C–O–C antisymmetric stretching, ring asymmetric stretching, and C–O stretching, respectively [16]. The large band at 1635 cm^{-1} is related to he OH bending of water tightly absorbed by the cellulose. The emergence of a new peak at 1740 cm^{-1} for modified CNC provided clear evidence of grafting by esterification of surface hydroxyl groups by the acid chloride. In addition to the typical C=O stretching band, other peaks at 1460, 2869, and 2927 cm^{-1} relative to CH_2 groups of the alkyl moiety are visible in the spectra of modified CNC. Intensification of these bands when moving from hexanoyl chloride to stearoyl chloride is consistent with the increase in the alkyl length of the grafted moiety. Although the grafting reaction should be limited to the external surface, the C=O band is relatively intense in the FTIR spectra. This result might be rationalized by two facts: first, the nanometric size of the CNC leads to a substantial loss of the number of hydroxyl groups exposed on the surface. For a CNC 6 nm wide, the surface hydroxyl groups account for more than 20 % of those of the whole sample. The second reason is the large proportion of the surface hydroxyl groups involved in the esterification reaction. This will be confirmed later by calculation of the DS on the basis of elemental analysis.

In an attempt to obtain more accurate information about the extent of surface functionalization, the CNC from data palm were modelled as a single crystal of type I cellulose with a square section of 6 nm in which the cellulose chains lie parallel to the (110) and $(1\bar{1}0)$ planes. Assuming average values of 0.54 and 0.61 nm between

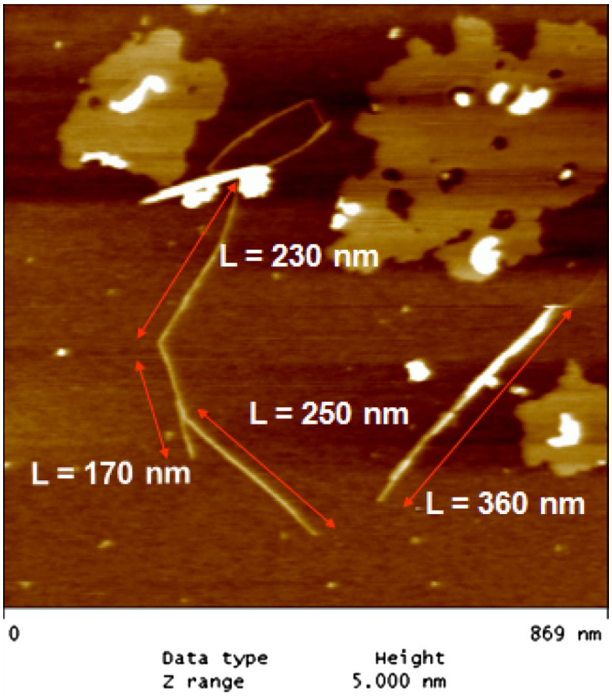

Fig. 1 AFM observation of CNC extracted from the rachis of the date palm tree

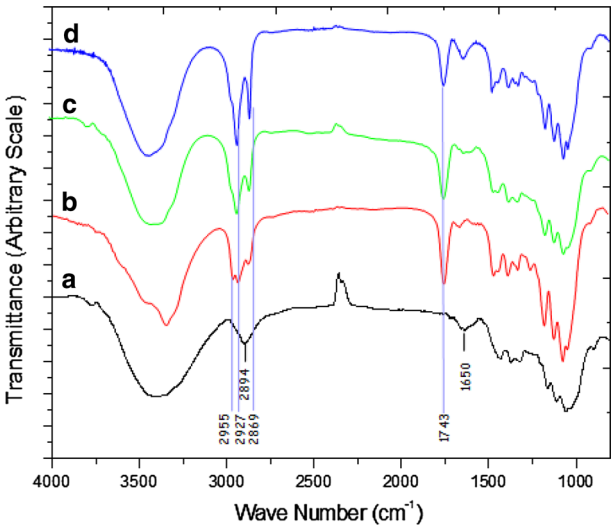

Fig. 2 Comparative FTIR spectra (KBr pellets) of unmodified CNC (*a*) and nanocrystals surface-modified with hexanoyl chloride AG6 (*b*), lauroyl chloride AG12 (*c*) and stearoyl chloride AG18 (*d*) after Soxhlet extraction

cellulose chains within the (110) and $(1\bar{1}0)$ faces, respectively, of the cellulose crystal, then, within this average crystal, the ratio of surface chains to the total number of chains inside the crystals can be calculated by use of the equation:

$$R = \frac{N \text{ surface chains}}{N \text{ chains in the crystals}} = \frac{2 \times (6/0.61 + 6/0.54)}{(6 \times 6)/(0.61 \times 0.54)} = 0.38 \tag{5}$$

Assuming that only the surface hydroxyl groups are involved in the coupling reaction, and considering that only 1.5 hydroxyl groups per anhydro glucose unit (AGU) of the surface layer are accessible to the reagent, the others being buried in the core of the crystalline domains, the maximum theoretical degree of surface substitution $DS_{S-max-max}$ likely to be achieved will be $1.5R$. Accordingly, the overall DS that can be achieved if all the accessible surface hydroxyl groups of the CNC are involved in the esterification reaction will be $DS = DS_{S-max} \times R = 0.57 \pm 0.07$.

Elemental analysis was performed to further confirm the occurrence of the grafting reaction in high yield and to obtain more precise information about the DS achieved. Indeed, according to Vaca-Garcia et al. [17], it is possible to calculate the DS, with good accuracy, on the basis of the result of elemental analysis by use of the equation:

$$DS = \frac{5.13 - 11.56 \times C}{C - 0.856 \times n + n \times C} \tag{6}$$

where C is the percentage of carbon in the sample and n is the number of carbon atoms in the acyl substituent.

From the data collected in Table 1 it is apparent that the DS values calculated by use of Eq. (2) ranged between 0.35 and 0.43. On the basis of the above reasoning

and use of Eq. (1), this led to a degree of substitution at the surface, DS_S, in the range 0.92–1.13. One can infer that each cellobiose unit (composed of two anhydroglucose units) on the CNC surface is grafted with at least one acyl chain, presumably one is coupled with the primary OH in the C6 carbon of the AGU and the second is linked with a secondary OH of the second AGU unit. In fact, considering that acyl chains bearing between 6 and 18 carbons adopt a stretched configuration with all the C–C being in the *trans* conformation, and taking into account a van der Waals radius of 1.7 Å for the carbon atom (http://www.ccdc.cam.ac.uk/products/csd/radji/table.php4), we might assume the acyl moiety is held within a cylinder 4.3 Å in diameter. Given that the distance between the O1 and O3 oxygen of the AGU unit is 5.5 Å, then, because of steric constraint, it is impossible for each AGU unit of the CNC surface to anchor more than one long acyl moiety. The configuration of the grafted chains on the surface of CNC is depicted schematically in Fig. 3. This reasoning may rationalize the fact that the maximum DS likely to be achieved by grafting of this CNC with long acyl chains could not exceed 0.4, irrespective of the reactivity of the grafting agent or its stoichiometric ratio. This corresponds to a maximum surface DS_s of 1.

Conversely, a slight decrease of approximately 10 % in the DS is apparent as the length of the grafted alkyl chains reaches 18 carbons. It is likely that the steric effect arising from the octadecyl moiety might bring about some restriction in the accessibility of the surface hydroxyl groups. However, one should note that the decrease in DS is modest.

XPS analysis was performed to more information about the conformation of the grafted chains on the surface of the CNC. The broad spectra obtained from the pristine and modified CNC contained the two peaks expected for oxygen and carbon atoms at approximately 532 and 285 eV, respectively. The C1s regions of the XPS spectra of the cellulose samples were fitted with four components C1, C2, C3, and C4 by use of curve fitting software (Spectrum NT). Peaks C1, C2, and C3 were assigned to aliphatic carbon at 285 eV; C–O and O–C–O cellulose carbon peaks were centred at 286.73 and 288.0 ± 0.2 eV, respectively. The C4 peak at 288.9 ± 0.2 eV was attributed to O–C=O of the grafted ester moiety (Fig. 4). Quantitative results are listed in Table 2.

From the atomic concentration of the different species at the surface one can estimate the degree of surface substitution as follows. The cellulose peak results from the contribution of five C–O bonds from the ring (two within the ring and three

Table 1 Elemental analysis of CNC before and after chemical modification with hexanoyl, lauroyl, and stearoyl chloride

	%C	%H	%O	%O/%C	DS
WRPd	41.22	6.34	51.44	1.247	–
WAG6	50.20	7.44	42.10	0.839	0.43
WAG12	54.12	8.31	36.56	0.633	0.45
WAG18	57.90	9.27	32.40	0.559	0.36

DS degree of substitution

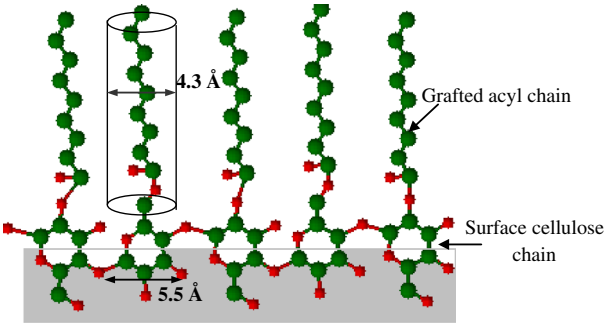

Fig. 3 Schematic model illustrating the surface arrangement of the grafted acyl chains on the surface of CNC after modification with acid chloride (the Van der Waals size of the alky chain and distance between the O1 and O3 were determined by use of ACD/Labs software)

from alcohol groups, irrespective of whether or not they are substituted) and one O–C–O group. The O–C=O arises from the grafted acyl moiety. The degree of surface substitution (DS_S) can be estimated by use of Eq. (7):

$$DS = \frac{O{-}C{=}O}{C_{cellulose}/6} \tag{7}$$

However, bearing in mind that the analysis depth of XPS is limited to approximately 30–40 Å, this led to consideration of the DS value from XPS as an estimate of the degree of substitution of the cellulose surface layer of CNC (DS_s). From the data in Table 2, we note that the DS_S values calculated on the basis of XPS analysis are approximately 0.7, slightly lower than those calculated on the basis of elemental analysis, which were found to be approximately 1. This difference may result from the contribution of two effects:

1 the first arises from the fact that in XPS the quantitative analysis encompasses, in addition to the top layer, the contribution of lower layers, but to a lesser extent; and
2 the second arises from the stretched configuration of the grafted acyl chains leading to some attenuation of the photoelectron from the surface cellulose layer.

The latter hypothesis is more obvious given the high density of the grafted alky chains on the surface, rendering their crowding more likely to occur. The increase in the $C1/C_{cellulose}$ ratio when moving from hexyl to octadecyl chloride is also indicative of the increased thickness of the layer on CNC as the length of the acyl moiety is increased. It also supports the hypothesis of a stretched conformation of the grafted acyl groups.

Contact angle measurements of liquid droplets on the surface of CNC after being mildly pressed into the form of a pellet to provide a uniform surface were performed to furnish information about evolution of the hydrophilic and/or hydrophobic character induced by the different surface modifications. The dynamic changes of the contact angle versus time for a drop of water are shown in Fig. 5. The low

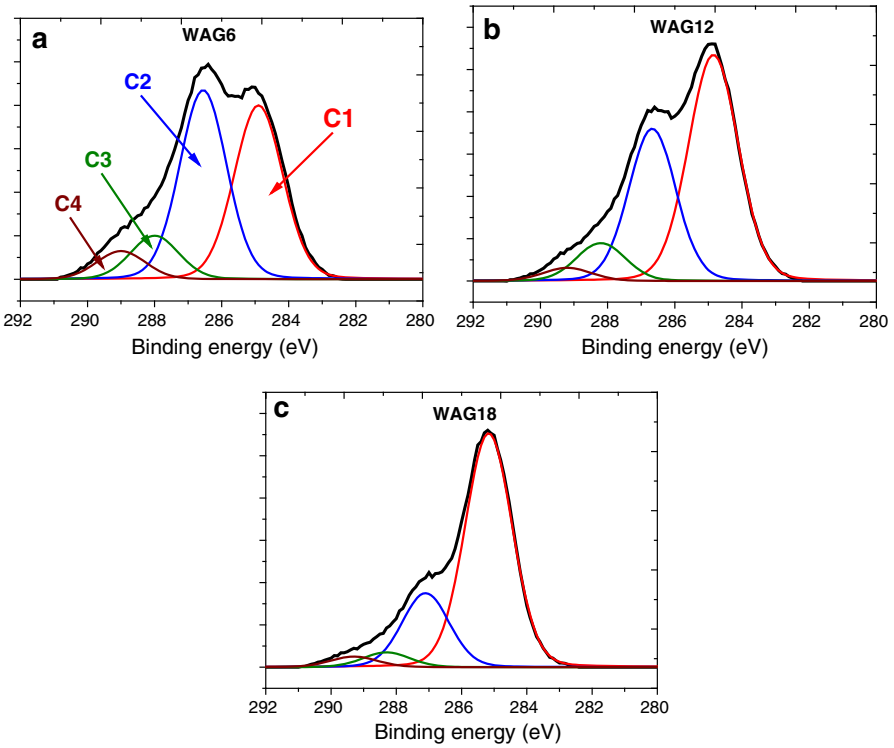

Fig. 4 Decomposition of the C1s signal into its constituent contributions for CNC grafted with **a** hexanoyl chloride, **b** lauroyl chloride, and **c** stearoyl chloride

Table 2 XPS analysis of CNC before and after surface chemical modification with hexanoyl, lauroyl, and stearoyl chloride

	C1 C–C, C–H	C2 C–O	C3 O–C–O, C=O	C4 O–C=O	$DS_{XPS} =$ $O - CO/C_{cll}/6$
Binding energy (eV)	285 ± 0.1	286.6 ± 0.1	288.1 ± 0.1	289.1 ± 0.1	
WAG6	40.5	42.8	10.1	6.6	0.75
WAG12	56.9	29.8	8.8	4.5	0.7
WAG18	70.2	22.2	4.4	3.1	0.7

contact angle value of the original CNC, approximately 45°, is consistent with the hydrophilic character of the surface as a consequence of the high density of surface hydroxyl groups on the CNC. After grafting with hexyl chloride, dodecyl chloride, and octadecyl chloride, the contact angle reached 90°, 100° and 109°, respectively, denoting a highly hydrophobic surface, which is a sign that the long aliphatic chains thoroughly hide the cellulose surface hydroxyl groups. Moreover, one should note the higher contact angle of approximately 110° in the presence of the octadecyl chain containing 18 carbon atoms; this is indicative of an ultra-hydrophobic surface.

There are two reasons for this character. First, the high DS leads to complete concealment of the surface hydroxyl groups on the CNC surface; second, the high structural order of the grafted C_{18} moiety results in formation of a tightly packed monolayer with methyl groups all pointing toward the surface. Such high contact angles approach those observed for densely packed monolayers of simple *n*-alkanethiols with $n > 16$ and with terminal (CH_3) groups adsorbed on gold [18].

To quantify the change of the surface energy as a consequence of surface modification, we measured the contact angles using four liquid probes—water, formamide, ethylene glycol, and diiodomethane. By applying the Owens and Wendt approach [19], both the dispersive and the polar contributions to the surface energy of these materials were calculated by use of Eq. 1. The results of this analysis are collected in Table 3.

Untreated CNC had its well-known high-polarity and dispersive energy values consistent with its hydrophilic character. The surface modification led to a huge decrease in the polar component consistent with evolution of the surface property from hydrophilic to hydrophobic character. The analysis was also indicative of quite a high value of γ for an acyl chain containing six carbon atoms, compared with chains containing 16 or 18 carbon atoms, for which γ_s^p was very close to 0. This means that CNC modified with dodecyl chloride or octadecyl chloride had almost no polar surface energy, which again indicates that the acyl chains totally masked the surface hydroxyl groups and imposed their own surface properties. The values of γ_s^d remained almost unchanged after modification with hexyl chloride and increased by approximately 30 % after modification with octadecyl chloride.

Coupling of long chains amines with CNC

Grafting of amines on to the CNC was performed for two reasons:

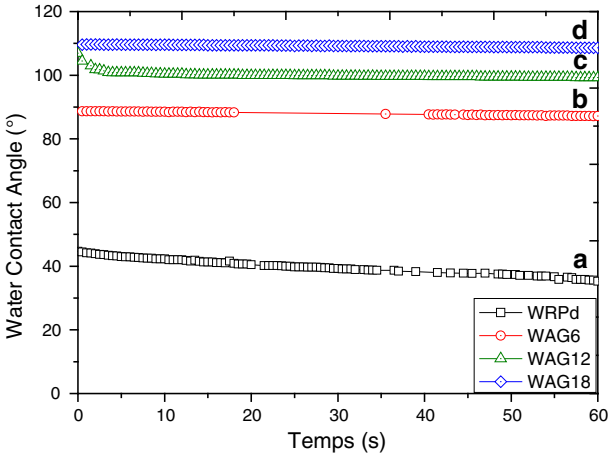

Fig. 5 Time evolution of the water contact angle with unmodified CNC (*a*) and CNC modified with hexanoyl chloride (*b*), lauroyl chloride (*c*) and stearoyl chloride (*d*)

Table 3 Surface energy contribution and contact angle values of the tested liquids for ungrafted and grafted CNC

Sample	Contact angle (°)			γ_S^p (mJ/m^2)	γ_S^d (mJ/m^2)	γ^S (mJ/m^2)
	Water	Ethylene glycol	Diiodomethane			
WRPd	42 ± 2.2	44 ± 1.2	52 ± 0.2	32.9	21.3	53.3
WAG6	92 ± 2.2	76 ± 1.4	54 ± 4.0	2.99	23.4	26.4
WAG12	104 ± 3.2	80 ± 0.7	56 ± 2.4	0.13	27.3	27.5
WAG18	108 ± 1.7	81 ± 0.2	55 ± 0.2	0.04	29.7	29.8

– first, to direct the grafting reaction toward a selective site on the surface; and
– second, was perform the modification in aqueous medium thus avoiding the need to remove the CNC from water.

The first step in the modification sequence was creation of carboxyl groups to enable coupling via the EDS/NHS approach [20]. For this purpose, TEMPO-mediated oxidation was accomplished. The emergence of the CO band at 1,740 cm^{-1} is consistent with occurrence of an oxidation reaction converting the primary hydroxyl groups on the surface to CNC–COOH.

On the basis of conductimetric titration, the DO achieved under the oxidation conditions was 0.2. If one uses reasoning similar to that in the previous section, but with the consideration that only one half of the primary surface hydroxyl groups (in C6) are accessible to oxidation, the others being buried inside the crystalline nanocrystal, then the maximum degree of oxidation (DO_{max}) that can be achieved for CNC is $DO_{max} = 0.38/2 = 0.19$. Therefore, it can be concluded that all the of the accessible surface hydroxymethyl groups have been carboxylated. To be sure that no aldehyde groups are present on the surface of the oxidized CNC, some of the oxidized CNC was further oxidized with $NaClO_2$ at pH 4–5; no increase in carboxyl groups was observed.

FTIR spectra acquired after reaction with amine are mainly characterized by a decrease in the CO band at 1740 cm^{-1} relative to the carboxyl function and the emergence of two new bands at 1640 and 1550 cm^{-1} typical of amide I and amide II (Fig. 6). The new bands, associated with C=O stretching and N–H bending vibration, respectively, are indicative of the occurrence of a condensation reaction between the amine and the carboxyl function. Further confirmation of the occurrence of the grafting reaction is attested by the increase in the nitrogen content, which reaches 1–1.5 % after interaction with the aminoalkane.

On the basis of the nitrogen content, it is possible to estimate the DS of the aminoalkane by use of the equation [17]:

$$DS = \frac{11.57N}{1 - N(n + 0.857)} \tag{8}$$

where N is the percentage of nitrogen in the sample and n is the number of carbon atoms in the acyl substituent.

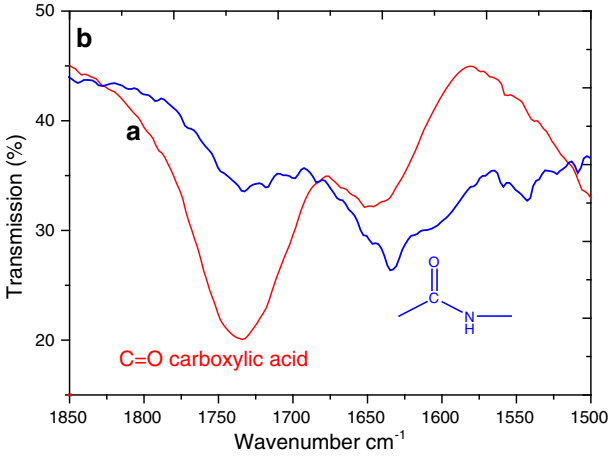

Fig. 6 FTIR spectra of CNC in the range 1500–1800 cm^{-1} after (*a*) oxidization (WOX) and (*b*) grafting with octadecylamine (WA18)

From the data collected in Table 4 it is apparent that DS_S calculated by use of Eq. (4) is higher for a C3 or C8 amine than for a C12 or C18 amine. For a C3 amine the DS of 0.2 indicates that all the carboxyl groups generated by the TEMPO-mediated oxidation reaction were involved in the coupling reaction with the amine. In all instances the maximum DS likely to be reached could not exceed DO_{max}. This explains why it is not possible to achieve the DS observed by modification with acid chloride. However, as the acyl chain length of the amine exceeds C8, the yield of the coupling reaction notably decreases and seems to level off at approximately 0.05 which corresponds to a DS_s of 0.14. This means that one in seven AGU units is grafted with acylamine. The less efficient coupling of alkaneamines bearing more than 12 carbon atoms might be related to the decrease in the solubility of the amine in the reaction medium.

Further confirmation of the grafting reaction was obtained by use of XPS, because the wide spectra revealed the presence of nitrogen. High-resolution C1s spectra provided more detail about the chemical environment of the carbon in the outer layer. In particular, the increase in the C–C/C–H contribution, with acyl length C12 or C18, with the emergence of a C–N peak at the expense of O–C=O is consistent with occurrence of the grafting reaction. From the quantitative data collected in Table 5 and Fig. 7 the degree of oxidation (DO_s) and degree of substitution (DS_s) at the surface can be estimated as follows:

$$DO_S = \frac{O-C=O}{C_{cellulose}/6} \tag{9}$$

$$DS_S = \frac{C-N}{C_{cellulose}/6} \tag{10}$$

From the XPS data, the surface DO_S was found to be near 0.5, meaning that half of the AGU units on the surface carried a COO^- group. This is to say, all the

Table 4 Elemental analysis of CNC before and after chemical modification by use of aliphatic amines

	%C	%H	%O	%N	%O/%C	%N/%C	DS
WRPd	41.22	6.34	51.44	0	1.247	0	–
WOX	39.66	6.04	53.97	<0.3	1.361	<0.008	–
WA3	43.06	6.95	48.25	1.67	1.120	0.040	0.26
WA8	41.99	6.34	50.68	0.92	1.207	0.023	0.11
WA12	42.98	6.41	49.68	0.86	1.156	0.021	0.05
WA18	48.48	7.92	41.81	1.70	0.862	0.036	0.06

DS degree of substitution

Table 5 Surface functional group composition obtained by deconvolution of the C1s signal with average binding energy position

	C1 C–C, C–H	C1′ C–N	C2 C–O	C3 O–C–O	C4 O–C=O	DS_{XPS}
Binding energy (eV)	285.0 ± 0.1	285.7 ± 0.1	286.6 ± 0.1	288.1 ± 0.1	289.1 ± 0.1	
WRPd-O	23.5 %	–	44.5 %	26.4 %	5.5 %	0.45[a]
WA8	26.3 %	6.1 %	51.2 %	15.3 %	1.1 %	0.54
WA12	44.4 %	1.5 %	42.1 %	11 %	0.9 %	0.16
WA18	45.2 %	1.7 %	40.3 %	11 %	1.7 %	0.2

[a] DO

accessible hydroxymethyl groups were oxidized, which is in good agreement with the theoretical value calculated above (DO_{max}). It is worth noting the quite good correlation between the DS value based on the elemental analysis and DS_S calculated on the basis of XPS, except for the C8 amine. Indeed, taking into account the relationship between DS and DS_S ($DS_S = DS/R = DS/0.38$), DS calculated on the basis of XPS data led to values of 0.2, 0.06, and 0.07 for C8, C12, and C18 amines, respectively.

The evolution of contact angle versus time for a drop of water after surface modification by amine grafting is shown in Fig. 8. As was observed after grafting with fatty acid chloride, modification of the CNC resulted in hydrophobic materials with contact angles of 84°, 86°, and 92° after grafting of propylamine, dodecylamine, and octadecylamine, respectively. These results seem unexpected, bearing in mind the lower grafting yield on the surface—for dodecylamine and octadecylamine only ~1 AGU unit undergoes coupling with amine. This discrepancy could be explained by considering that the acyl chains of the grafted amine lie parallel to the surface, enabling concealment of a high fraction of the surface hydroxyl groups.

Quantitative evolution of the surface properties after amine grafting is further emphasized by the huge decrease in the polar component γ_p of the value the surface energy. As shown in Table 6, γ_p drops to 2 mJ/m^2 after modification with octylamine and octadecylamine whereas the dispersive component γ_d remains almost unchanged.

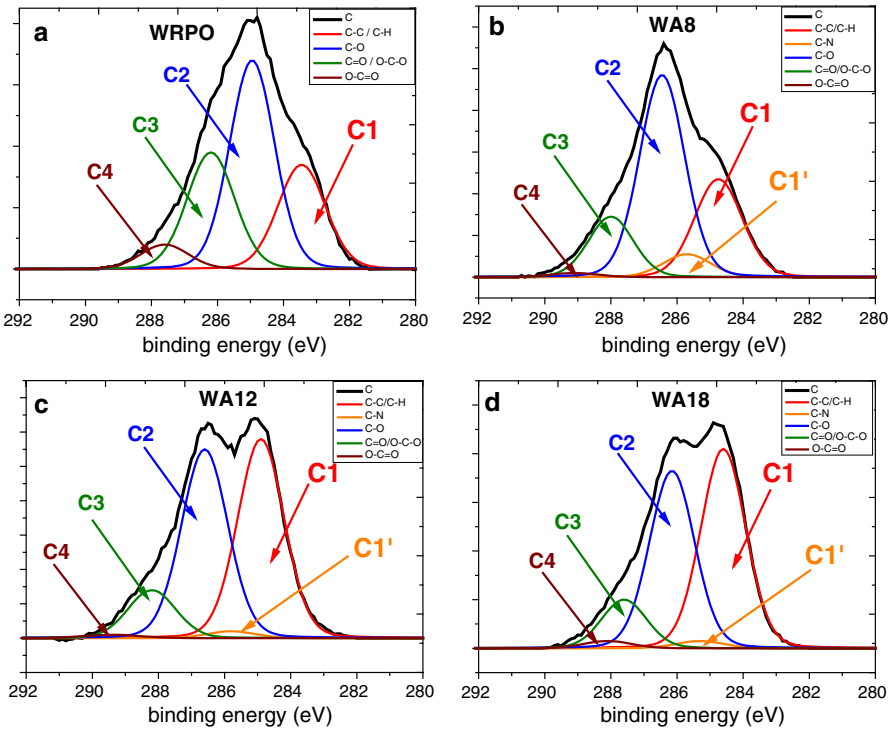

Fig. 7 Deconvolution of the C1s signal into its constituent contributions for oxidized CNC (**a**) and oxidized CNC coupled with A8 (**b**), A12 (**c**) and A18 (**d**)

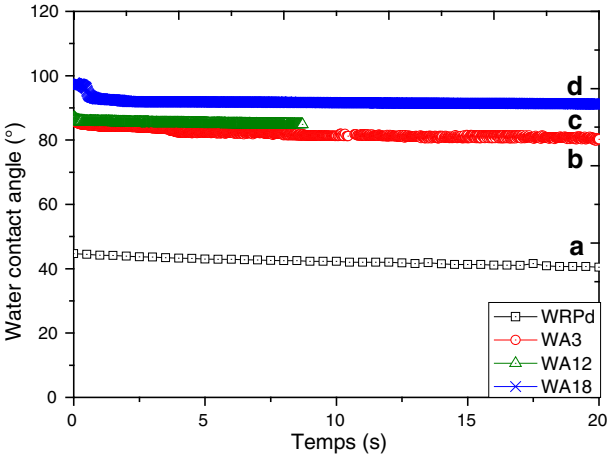

Fig. 8 Water contact angle versus time for unmodified CNC (*a*) and CNC modified with *n*-octylamine A8 (*b*), dodecylamine A12 (*c*), and octadecylamine A18 (*d*)

Table 6 Surface energy contribution and contact angle values of the tested liquids for ungrafted and grafted CNC

Sample	Contact angle			γ_S^P (mJ/m^2)	γ_S^d (mJ/m^2)	γ_S (mJ/m^2)
	Water	Ethylene glycol	Diiodomethane			
WRPd	42 ± 2.2	44 ± 1.2	52 ± 0.2	32.9	21.3	53.3
WA8	92 ± 2.3	55 ± 1.3	59 ± 0.9	2	30	32
WA18	94 ± 4.0	80 ± 1.6	67 ± 1.6	3	20	23

Conclusion

Surface modification of CNC by grafting of long aliphatic chains has been achieved by two different strategies—esterification with acid chloride and amidification with aliphatic amine using the EDC/NHS approach. The former reaction was performed in toluene, after solvent exchanges of water; the latter was performed directly in aqueous medium without any need to remove water from the CNC. Grafting efficiency was apparent from FTIR and XPS spectroscopy and elemental analysis. On the basis of this analysis and the size of the CNC, the DS was calculated; from this it was possible to obtain a clear idea about the density of grafting on the surface. It was shown that complete esterification of all the accessible hydroxyl groups on the surface of the CNC was achieved, irrespective of whether they were primary or secondary, when the reaction was performed with acid chlorides. In contrast, reaction with alkylamine after surface-mediated oxidation enabled selective orientation of the grafting reaction solely on carboxyl groups arising from selective oxidation of the C6 OH groups. However, the grafting yield was lower in the presence of octylamine and octadecylamine. Irrespective of the method of modification, the surface was hydrophobic after modification, especially for acyl chains with 18 CH_2 groups.

Acknowledgments The authors are grateful for financial support from the Hassan II Academy of Sciences and Technologies, the French Ministry of Foreign Affairs (Corus program 6046), the Agence Universitaire de la Francophonie (AUF, Projet de Coopération Scientifique Inter-Universtaire), and the Morocco–Tunisia committee for scientific cooperation.

References

1. M.A.S. Azizi Samir, F. Alloin, A. Dufresne, Biomacromolecule **6**, 612–626 (2005)
2. V. Favier, H. Chanzy, J.Y. Cavaille, Macromolecules **28**, 6365–6367 (2005)
3. N. Lin, J. Huang, A. Dufresne, Nanoscale **4**, 3274–3294 (2012)
4. S.J. Eichhorn, A. Dufresne, M. Aranguren, N.E. Marcovich, J.R. Capadona, S.J. Rowan, C. Weder, W. Thielemans, M. Roman, S. Renneckar, W. Gindl, S. Veigel, J. Keckes, H. Yano, K. Abe, M. Nogi, A.N. Nakagaito, A. Mangalam, J. Simonsen, A.S. Benight, A. Bismarck, L.A. Berglund, T. Peijs, J. Mater. Sci. **45**, 1–33 (2010)
5. H. Yuan, Y. Nishiyama, M. Wada, S. Kuga, Biomacromolecules **7**, 696–700 (2006)
6. S. Berlioz, S. Molina-Boisseau, Y. Nishiyama, L. Heux, Biomacromolecules **10**, 2144–2151 (2009)
7. C. Gousse, H. Chanzy, G. Excoffier, L. Soubeyrand, E. Fleury, Polymer **43**(2002), 2645–2651 (2002)
8. G. Siqueira, J. Bras, A. Dufresne, Langmuir **26**, 402–411 (2010)

9. W. Thielemans, M.N. Belgacem, A. Dufresne, Langmuir **22**, 4804–4810 (2006)
10. G. Morandi, L. Heath, W. Thielemans, Langmuir **25**, 8280–8286 (2009)
11. J.O. Zoppe, Y. Habibi, O.J. Rojas, R.A. Venditti, L.S. Johansson, K. Efimenko, M. O"sterberg, J. Laine Biomacromol. **11**, 2683–2691 (2010)
12. A.L. Goffin, J.M. Raquez, E. Duquesne, G. Siqueira, Y. Habibi, A. Dufresne, P. Dubois, Biomacromolecules **12**, 2456–2465 (2011)
13. A. Bendahou, Y. Habibi, H. Kaddami, A. Dufresne, J. Biobased Mat. Bioenergy **3**, 1–10 (2009)
14. J.F. Watts, J. Wolstenholome, *An Introduction to Surface Analysis by XPS and AES* (Wiley, Chichester, 2003)
15. C.A. Cateto, A. Ragauskas, RSC Advances **1**(2011), 1695–1697 (2011)
16. C.Y. Liang, R.H. Marchessault, J. Polym. Sci. **39**, 269–278 (1959)
17. C. Vaca-Garcia, M.E. Borredon, A. Gaseta, Cellulose **8**, 225–231 (2001)
18. E.B. Troughton, C.D. Bain, G.M. Whitesides, Langmuir **4**(1988), 365–385 (1988)
19. D.K. Owens, R.C. Wendt, J. Appl. Polym. Sci. **13**, 1741–1747 (1969)
20. C. Zhang, N. Luo, D.E. Hirt, Langmuir **22**, 6851–6857 (2006)